

Barcoded Microchips for Biomolecular Assays

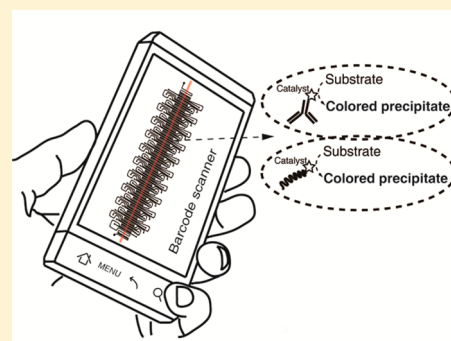
Yi Zhang,^{†,‡} Jiashu Sun,^{*,†} Yu Zou,[‡] Wenwen Chen,[†] Wei Zhang,^{*,†} Jianzhong Jeff Xi,[‡] and Xingyu Jiang^{*,†}

[†] Beijing Engineering Research Center for BioNanotechnology & CAS Key Laboratory for Biological Effects of Nanomaterials and Nanosafety, National Center for Nanoscience and Technology, Beijing 100190, China

[‡] Department of Biomedical Engineering, College of Engineering, Peking University, Beijing 100871, China

S Supporting Information

ABSTRACT: Multiplexed assay of analytes is of great importance for clinical diagnostics and other analytical applications. Barcode-based bioassays with the ability to encode and decode may realize this goal in a straightforward and consistent manner. We present here a microfluidic barcoded chip containing several sets of microchannels with different widths, imitating the commonly used barcode. A single barcoded microchip can carry out tens of individual protein/nucleic acid assays (encode) and immediately yield all assay results by a portable barcode reader or a smartphone (decode). The applicability of a barcoded microchip is demonstrated by human immunodeficiency virus (HIV) immunoassays for simultaneous detection of three targets (anti-gp41 antibody, anti-gp120 antibody, and anti-gp36 antibody) from six human serum samples. We can also determine seven pathogen-specific oligonucleotides by a single chip containing both positive and negative controls.



The realization of accurate and multiplexed biochemical assays without resorting to advanced diagnostic tools remains challenging to chemists, biologists, and engineers. Microfluidic technology has been adopted for multiplexed assays with additional benefits, including reduced sample/reagent consumption, shortened assaying time, and enhanced flexibility.^{1,2} However, few studies have made a real impact due to the lack of a portable, cost-effective, sensitive, and reliable readout system for the miniaturized microfluidic chip.^{3–8} Although a few pioneering studies employed commercialized personal healthcare devices such as the glucose meter for rapid analysis of biomarkers, they were still limited in the ability of multiplexing.^{9,10}

As a symbol of modern technology, barcodes can store and organize a large amount of data by arranging dark bars and light spaces with different widths, allowing for different combinations to represent different information. Similarly, the most common form of the output of a diagnostic test is “yes/no” binary information, just like the “bar” and the “space” in the barcode. Some researchers have used the “barcode” concept (so far all in the metaphorical, not literal, sense of this word) in biomedical diagnostics for multiplexing,^{11,12} such as compositional encoding,¹³ shape-encoding,^{14,15} color-encoding,^{16–18} wavelength- and light-intensity-encoding,^{19–23} dot-encoding,²⁴ radio-frequency-encoding,²⁵ and genetic encoding.²⁶ These methods require either complicated synthesis to generate the barcode as tags for labeling or complex instrumentation for readouts, such as reflectance microscopy,^{13,16,18,27} fluorescence microscopy,^{19,22,24,26,28} atomic force microscopy,²⁹ and spectroscopy.^{19,23,30,31} These complex approaches restrict barcode-based analytical systems from being widely applied for clinical

diagnostic or analytical applications. Moreover, the growing needs increasingly call for the development of a barcoded bioassay system allowing for multiplexed detection of proteins/nucleic acids (encode) and straightforward/efficient readout (decode), just like traditional barcodes and barcode readers used in the supermarket.

In this work, we first design and fabricate a microfluidic barcoded chip according to barcode symbology specification. This barcoded microchip is employed for multiplexed human immunodeficiency virus (HIV) immunoassays or detection of several pathogen-specific oligonucleotides. The assay result of a maximum of 20 samples in a single barcoded chip can be directly analyzed by scanning the chip using the barcode reader/smartphone.

EXPERIMENTAL SECTION

Design of Microfluidic Barcoded Chips. A microfluidic barcoded chip for multiplexed protein/nucleic acid assays contains 1 long, serpentine microchannel through the whole barcode area, designated as C1, and 20 sets of short, vertical channels, designated as C2–C21 (Figure 1). Channel C1 serves as a positive control that ensures the integrity of a barcode which appears as dark bars after bioassays (constant region, colored in gray in Figure 1). Each of the 20 sets of vertical channels C2–C21 (variable region, 200 μm width for each channel, colored in red in Figure 1) consists of 2 identical channels filled with the

Received: July 21, 2014

Accepted: December 16, 2014

Published: December 16, 2014



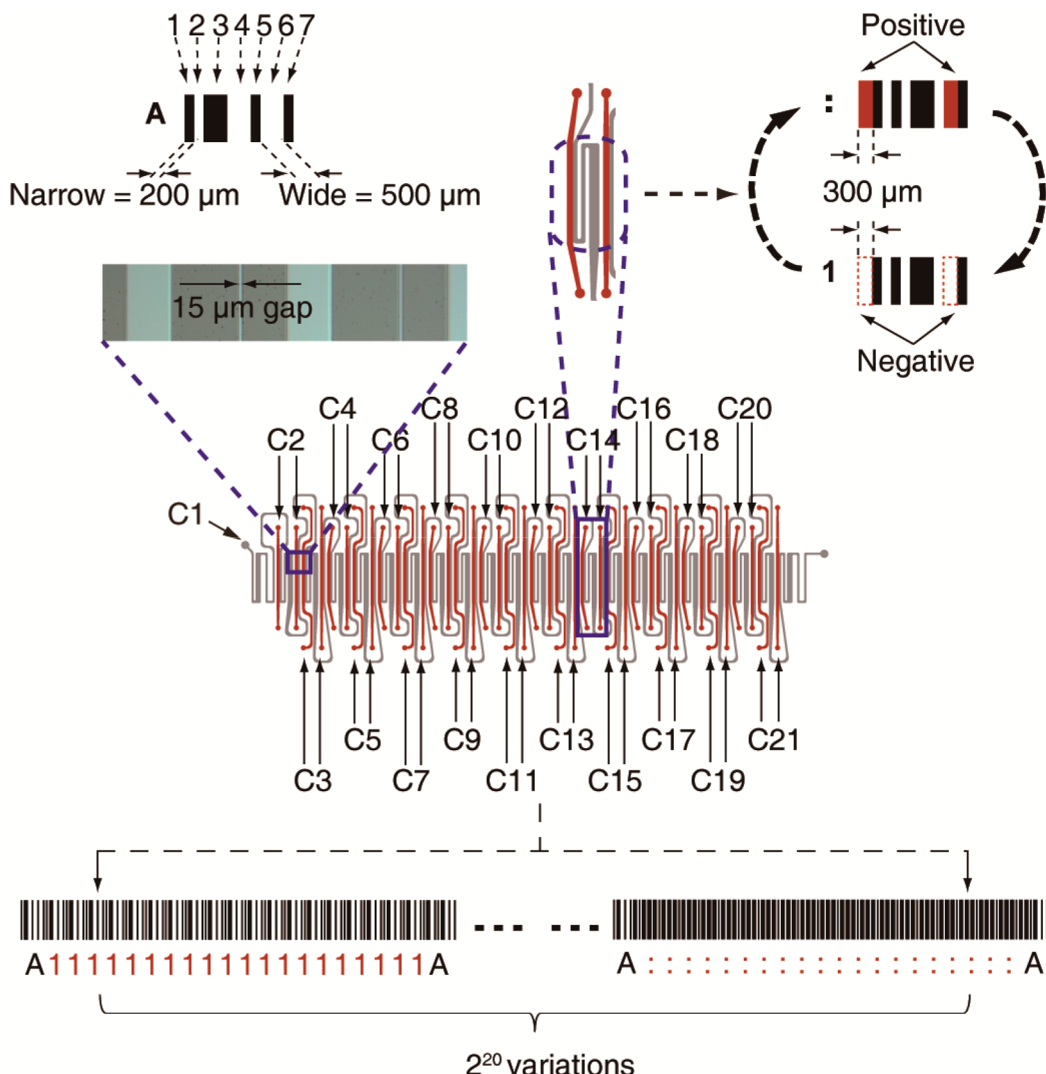


Figure 1. Design of microfluidic barcodes. The gray channel, C1, is the constant region displayed as dark bars after bioassays. The red channels, C2–C21, are variable regions filled with samples/solutions which could be either bars or spaces, depending on the positive or negative results of the assays. Each paired vertical channel (C2–C21) and a part of channel C1 form a variable Codabar symbol (“:” or “1”). If all samples in channels C2–C21 are positive, the barcode is read as “A::::::::::A”. If all samples are negative, the barcode is read as “A11111111111111111111A”. The magnified inset shows a part of the master with a small gap between the variable region and the constant region.

same sample solution. These paired C2–C21 channels also enable a parallel duplicate experiment required by general bioassays. Channels C2–C21 may appear as dark bars or light spaces depending on the positive or negative results of the assays. Each paired vertical channel C2–C21 and a part of channel C1 form a variable Codabar symbol (“:” or “1”) consisting of seven elements (four bars plus three spaces). The symbols “:” and “1” can be transformed from one to another, depending on the widths of the leftmost (element 1) and rightmost (element 7) elements, indicated by the red blocks and dashed red lines at the upper right side of Figure 1. If the samples in the vertical channels are positive, the channels will become bars and the symbol will display as “:”. If the samples are negative, the channels will remain as spaces and the symbol will display as “1” (Figure 1; movie S1, Supporting Information). The 20 variable symbols of either “:” or “1” along with two start/end symbols of “A” compose a Codabar barcode. If all samples in the 20 sets of vertical channels are positive, the microfluidic barcode will be read as “A::::::::::A”. In contrast, if all samples are negative, the barcode will be read as “A11111111111111111111A”. To

separate each reaction channel, tens of small gaps are designed along several millimeters in length (see the inset image in Figure 1). This gap cannot be too large; otherwise the gap itself will be mistakenly recognized as a space. This gap cannot be too small either, because of the limited precision of the photomask. We adopt a moderate 15 μm width for the gap, because the barcode reader does not treat the 15 μm gap as a space (it could be larger than 15 μm, but will potentially increase the chances of misreading) and the corresponding microfabrication is relatively simple and easy to repeat (i.e., the smaller size will increase the cost/difficulty of microfabrication). More design details can be found in the Supporting Information.

Protocol of HIV Immunoassay. The HIV immunoassay is carried out on the PDMS substrate covered with barcoded microchannels. Briefly, after loading the exact amount of samples/reagents into the pipet, we align the tip of the pipet with the inlet port of the barcoded chip and gently press the pipet to allow the sample/reagent to flow into the channel (movie S2, Supporting Information). The procedures are as follows:

(1) Introduce HIV surface antigens into barcoded microchip. Recombinant HIV-1 envelope gp41 antigen (abbreviated as gp41, 10 $\mu\text{g mL}^{-1}$, 1 μL for each channel) is introduced into microchannels C2, C5, C8, C11, C14, and C17. Recombinant HIV-1 gp120 nef mosaic antigen (abbreviated as gp120, 10 $\mu\text{g mL}^{-1}$, 1 μL for each channel) is introduced into C3, C6, C9, C12, C15, and C18. Recombinant HIV-2 gp36 antigen (abbreviated as gp36, 10 $\mu\text{g mL}^{-1}$, 1 μL for each channel) is introduced into C4, C7, C10, C13, C16, C19, and C21. Recombinant HIV-1 p17–p24 gp41–gp120 antigen (abbreviated as p17–p24 gp41–gp120, 10 $\mu\text{g mL}^{-1}$, 1 μL) is introduced into C20. All antigens are incubated for 20 min and then washed with PBST (phosphate-buffered saline, pH 7.2, containing 0.05% (v/v) Tween-20) three times.

(2) Block microchannels C2–C21. Channels are blocked with Detector Block (1% (w/v) powder, KPL) inside the channels for 10 min and washed with PBST three times.

(3) Introduce human serums into the barcoded microchip. Six serum samples (serum nos. 1–6, 20-fold dilution, 2 μL each) are introduced into C2–C4 (gp41 in C2, gp120 in C3, and gp36 in C4, as mentioned above), C5–C7, C8–C10, C11–C13, C14–C16, and C17–C19. A 2 μL volume of HIV (1 + 2) antibody-negative control is introduced into the C20 and C21 channels. After introduction, human serums are incubated for 20 min and washed with PBST three times.

(4) Introduce secondary antibody into the microchannels. Horseradish peroxidase-conjugated goat antihuman IgG (abbreviated as HRP–Go-a-Hu IgG, diluted by a secondary antibody dilution buffer, 1 μL for each channel) is introduced into the C2–C21 channels, and 15 μL of HRP–Go-a-Hu IgG diluted by PBS is introduced into the C1 channel. In C2–C21, the HRP–Go-a-Hu IgG can specifically bind to human immunoglobulins if human serum contains HIV antibodies, while in C1, HRP–Go-a-Hu IgG will nonspecifically adsorb onto the surface of the PDMS substrate. After incubation for 20 min and washing with PBST three times, the barcoded microchip is peeled from the PDMS substrate. The substrate is then washed again with PBST three times.

(5) Enzyme-catalyzed colorimetric reaction. The PDMS substrate containing the whole reaction region of the barcode is covered with the one-component 3,3',5,5'-tetramethylbenzidine (TMB) substrate (KPL), followed by incubation for 5 min or until the desired dark-blue color is developed. The HRP-catalyzed colorimetric reaction is stopped by removing the TMB substrate and washing with deionized water gently.

Protocol of Oligonucleotide Detection. The oligonucleotide detection is carried out on a poly-L-lysine-precoated glass substrate covered with barcoded microchannels. The procedures are as follows:

(1) Introduce oligonucleotides into the microchannels. All oligonucleotides (Table S1, Supporting Information) are synthesized by Sangon Biotech Co., Ltd. and diluted in deionized water. A 1 μL volume of 100 μM oligonucleotides is introduced into each microchannel C2–C21 as follows: ALF-CP (capture probe for anthrax lethal factor gene) into C2 and C3; BA-CP (capture probe for *Bacillus anthracis* protective antigen gene) into C4 and C5; EV-CP (capture probe for Ebola virus) into C6 and C7; Non (blank control of capture probe) into C8 and C9; HAV-CP (capture probe for hepatitis A virus Val17 polyprotein gene) into C10 and C11; HBV-CP (capture probe for hepatitis B virus surface antigen gene) into C12 and C13; HIV-CP (capture probe for human immunodeficiency virus) into C14 and C15; Non (blank control of capture probe) into C16 and C17; VV-CP

(capture probe for variola virus) into C18 and C19; Non (blank control of capture probe) into C20 and C21. The solution-filled chip is placed into a desiccator overnight at room temperature to allow water to evaporate completely through the inlet and the outlet, leaving the oligonucleotide molecules behind.

(2) Introduce oligonucleotides into the C1 microchannel. Gold nanoparticle (AuNP)-conjugated detection probes are diluted in 0.3 M PBS (pH 7.0), and the final concentration of each conjugate is about 0.5–1.0 nM. A mixture solution of AuNP–oligonucleotide conjugates is introduced into the C1 channel from the inlet to the outlet and incubated for 30 min. The solution is then removed from the outlet, followed by refilling the C1 channel with the same mixture solution from the outlet to the inlet (i.e., the reverse direction, Figure S1, Supporting Information), incubating the channel for 30 min, and removing the solution from the inlet. The dried chip is placed in an oven at 80 °C for 4 h.

(3) Block the C2–C21 channels with succinic anhydride. The C2–C21 channels are blocked with succinic anhydride blocking solution inside the channels for 15 min and washed with 0.02% (w/v) SDS and deionized water in turn. The chip is dried completely in a desiccator.

(4) Introduce oligonucleotide targets into the microchip. A mixture solution of all seven oligonucleotide targets (500 nM, diluted in 0.3 M PBS) is introduced into the C2–C15, C18, and C19 channels (1 μL each). C16, C17, C20, and C21 are the blank controls of target sequences and are only filled with the buffer solution. The target sequences can specifically bind with the immobilized capture probes. The barcoded microchip is incubated in a humid chamber for 4 h, followed by washing the microchannels with 0.3 M PBS and drying the chip in a desiccator completely.

(5) Introduce the AuNP-conjugated detection probe. A mixture solution of AuNP–oligonucleotide conjugates (i.e., the detection probes) is introduced into the C2–C7 and C10–C19 channels (1 μL each). The detection probes will either be immobilized on the surface of the glass slide or not, depending on whether the sample contains corresponding oligonucleotide targets. The barcoded microchip is incubated in a humid chamber for 2 h, followed by washing the microchannels with 0.01 M PBS (pH 7.0) to remove the nonspecific interactions. The barcoded microchip is peeled from the substrate, and the surface of the substrate is washed three times with 0.3 M NPBS (0.3 M NaNO₃, 10 mM NaH₂PO₄/Na₂HPO₄, pH 7.0).

(6) Silver enhancement. The substrate containing the whole reaction region of the barcode is covered with the silver enhancer solution and incubated for 3 min. The silver solution is then replaced by a freshly prepared, one and the substrate is further incubated for 3 min at room temperature. The reaction is stopped by removing the enhancer solution and washing the reaction region with deionized water gently.

Barcode Reading. In the case of PDMS as the substrate, we place the reacted barcode pattern on a piece of white paper or on a color card (in the case of track-etched polycarbonate (TEPC) membrane as the substrate, there is no need for this operation) to provide sufficient contrast between bars and spaces and decipher the barcode by a compact laser hand-held barcode reader (BL-N70UBE, Keyence) or a smartphone (Desire HD A9191, HTC) equipped with a built-in 8.0 megapixel CMOS (complementary metal oxide semiconductor) camera. For readout by the hand-held barcode reader, it emits and receives a laser (~650 nm) during the operation. A red status LED lights up when the laser emits, and a green status LED lights up when the barcode is read

correctly. A buzzer sounds after the reading is complete or after the acquired data are sent to the connected notebook or devices carrying word-processing software (movie S3, Supporting Information). For readout by the smartphone, we just bring the barcode within the viewfinder, and the mobile app that we develop will automatically focus and recognize the barcode and display the detected symbols on the screen of the smartphone (movie S3).

RESULTS AND DISCUSSION

Characterization of Barcoded Microchips. To seal PDMS onto the various surfaces, the microfluidic channels and

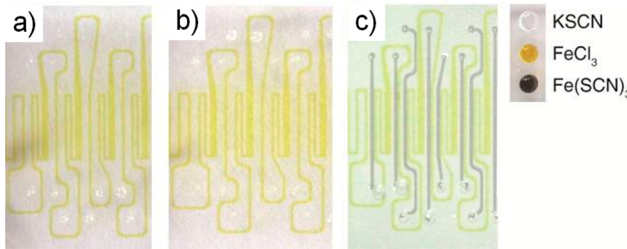


Figure 2. Contamination test for the quality control of microfluidic barcoded chips. The adjacent microchannels are separated by a $15\ \mu\text{m}$ gap. PDMS microfluidic channels are sealed with PDMS substrate (a), glass substrate (b), or TEPC membrane (c). A slightly gray color in the microchannels of (c) is observed, but this is due to the reflection of KSCN solutions absorbed on the surface of the TEPC membrane, not the leakage between neighboring microchannels.

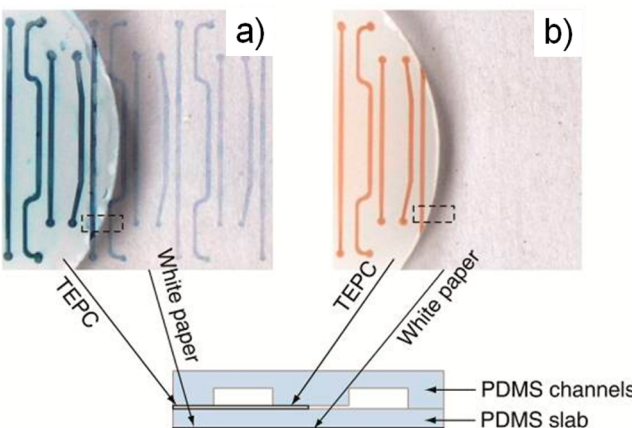


Figure 3. Comparison between the TEPC and PDMS substrates. The HRP-conjugated proteins could be visualized by color development with TMB (a) or DAB (b). TEPC could adsorb more proteins than PDMS.

PDMS, glass, or TEPC substrate are treated by oxygen plasma (PDC-002, Harrick Plasma Cleaner) for 5 s at low radio frequency. A handful of hydroxyl groups generated during the mild plasma treatment could provide the desired moderate bonding strength. Then we place the channels onto the substrate without further heating to form a reversible bonding. After assembly of the barcoded microfluidic chip, we perform the contamination test to prove a good bonding between the PDMS chips and different substrates, as well as no contamination between neighboring channels separated by the $15\ \mu\text{m}$ gap. The PDMS chips are sealed with PDMS substrate, glass substrate, or TEPC membrane substrate (0.2 μm pore size, Whatman, GE Healthcare). For each pair of sealed microchannels, one channel

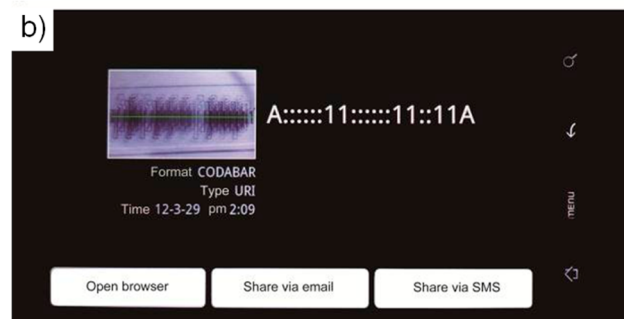
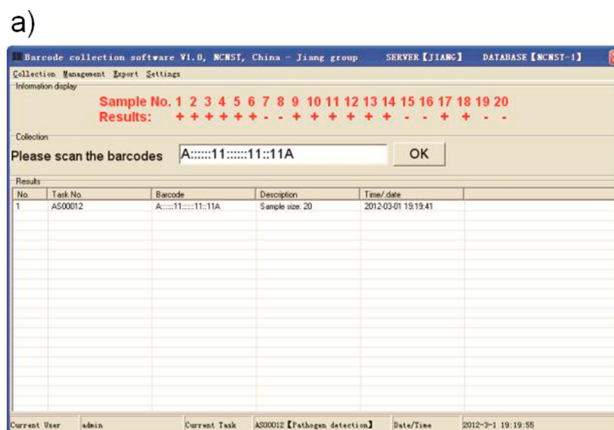


Figure 4. Software interface of barcode readers. (a) PC software. This software could collect and transform the barcodes and display the results of assays. "+" means positive; "-" means negative. (b) Mobile app. The barcode could be automatically recognized and displayed on the screen of the smartphone.

is filled by ferric chloride (FeCl_3 ; 0.80 M, yellow color) and the other channel is filled by potassium thiocyanate (KSCN; 5.14 M, colorless). This assay is very sensitive.³² If one of the liquids contacts the other one, a dark red or even black color will appear, resulting from the production of $\text{Fe}(\text{SCN})_3$. We observe that the neighboring microchannels separated by the $15\ \mu\text{m}$ gap remain yellow and colorless, respectively, indicating a good seal of PDMS with various substrates (Figure 2).

To test the ability of the TEPC membrane for protein adsorption, we sandwich the TEPC membrane (thickness 7–20 μm) between PDMS channels and a PDMS slab tightly. In this test, the TEPC membrane partially covers the barcode region, and we incubate the PBS-diluted HRP-conjugated antibody solution inside the microchannels for 20 min at room temperature, followed by PBST washing. We develop the colors using the TMB or 3,3'-diaminobenzidine (DAB) substrate. The results prove that the porous TEPC membrane could adsorb more proteins than the flat PDMS surface (Figure 3). Especially, DAB could only develop visible color on the TEPC substrate.

Decoding of Barcoded Microchips. The principle of the barcode reader is based on the differential reflectivity between dark bars and light spaces. Several widely used biochemical assays, e.g., the enzyme-linked immunosorbent assay (ELISA), could meet the above contrast requirement and generate a visible color change. Another example is the “gold label silver stain” method for visible detection of biomolecules.³³ According to the different labels and substrates, they can generate different products with different colors. We confirmed the readability of such colors in a barcode format (Table S2, Supporting Information).

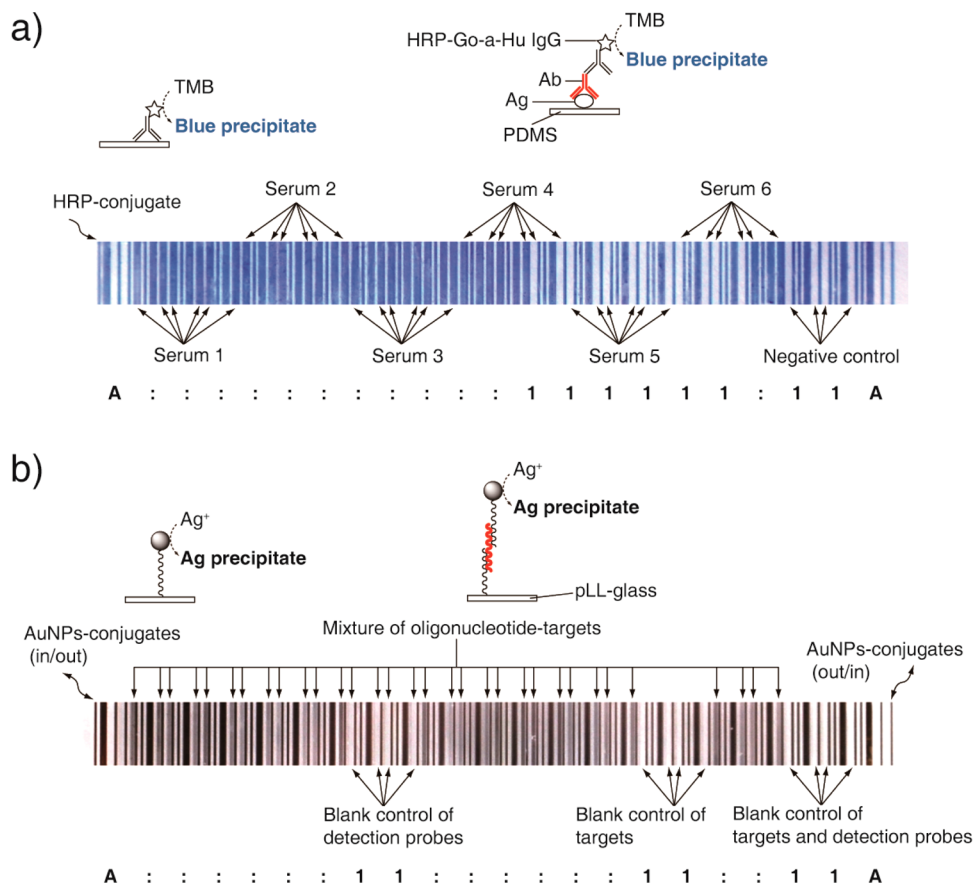


Figure 5. Analyses of biological molecules using the barcoded microfluidic chip. (a) HIV immunoassay detects three targets (anti-gp41 antibody, anti-gp120 antibody, and anti-gp36 antibody) from six human serum samples simultaneously. Each serum is detected in duplicate. (b) Sandwich hybridization of DNA detects seven pathogen-specific oligonucleotides in a mixture: ALF, BA, EV, HAV, HBV, HIV, and VV. Each target is detected four times in parallel.

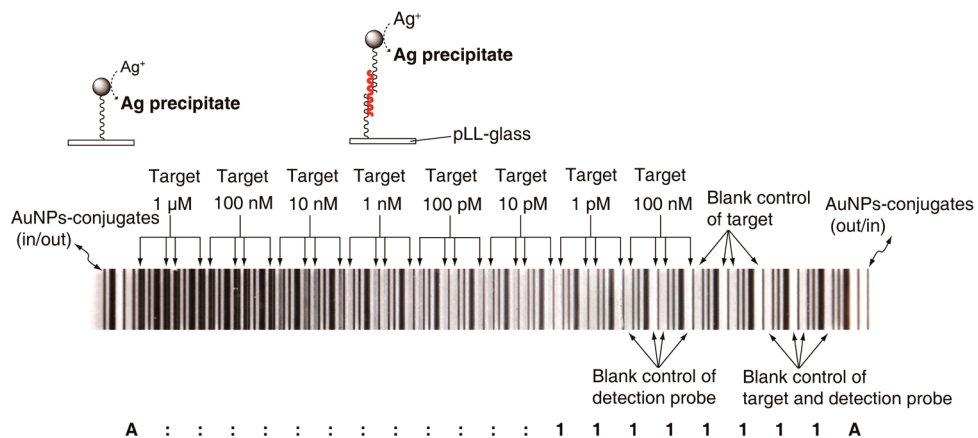


Figure 6. Determination of the LOQ using the barcoded microchip. The LOQ for HBV is 10 pM, since the corresponding channels are recognized as “.”

After acquisition of the barcode patterns produced from our experiments, we first use a compact laser hand-held barcode reader to read the barcode (see the Experimental Section). To make the readout straightforward to untrained users, we write a program which could collect data from the barcode reader and transform the symbols into a text showing the result of the assay (Figure 4a; movie S3, Supporting Information). We also develop a smartphone-based decoding. The basic principle is different from the barcode reader as it relies on digital image processing of a barcode pattern captured by a built-in camera on a smartphone

(Figure 4b; movie S3). Individuals performing bioassays in remote locations could send the results of the assays to off-site clinicians throughout the mobile network.

Barcoded Microchips for HIV Immunoassays. For protein analysis, we carry out HIV immunoassays for simultaneous detection of three targets from six human serum samples (details in the Experimental Section). Anti-gp41 antibody and anti-gp120 antibody are used as biomarkers for the diagnostics of the infection of HIV-1, and anti-gp36 antibody is for HIV-2. The result of the HIV test using the barcoded

microchip is shown in Figure 5a. Negative control samples at C20 (for HIV-1) and C21 (for HIV-2) are read as “1”. The positive control is HRP-conjugated antibody-filled C1, the long serpentine microchannel that runs throughout the barcode and is necessary for the integrity of the barcode. The barcode is read as “A::::::::::111111:11A” by the barcode reader immediately (within 1 s) after reaction. This pattern indicates that C2, C5, C8, and C11 are recognized as bars (i.e., the corresponding regions are read as “:”), so serums 1–4 are gp41 positive; C14 and C17 are recognized as spaces (i.e., the corresponding regions are read as “1”), so serums 5 and 6 are gp41 negative. Similarly, C3, C6, C9, and C12 are recognized as bars, indicating that serums 1–4 are gp120 positive, while C15 and C18 are recognized as spaces, yielding serums 5 and 6 gp120 negative. C4, C7, C10, and C19 (corresponding to serums 1–3 and 6) are recognized as bars, revealing the serums are gp36 positive; C13 and C16 are recognized as spaces, so serums 4 and 5 are gp36 negative. According to these results and WHO (World Health Organization) reports for detection of HIV (<http://apps.who.int/iris/handle/10665/43025>), we can determine that serums 1–3 are HIV-1/2 positive, serum 4 is HIV-1 positive and HIV-2 negative, serum 5 is HIV-1/2 negative, and serum 6 is HIV-1 negative and HIV-2 positive.

Barcoded Microchips for Oligonucleotide Detection.

Our system can also detect nucleic acids using AuNP-conjugated oligonucleotides followed by silver staining (details in the Experimental Section and Supporting Information). As a demonstration, we simultaneously detect seven pathogen-specific oligonucleotides (Table S1, Supporting Information), anthrax lethal factor (ALF), *B. anthracis* protective antigen gene (BA), Ebola virus (EV), hepatitis A virus Vall7 polyprotein gene (HAV), hepatitis B virus surface antigen gene (HBV), HIV, and variola virus (VV), from a mixture (Figure 5b). The barcode is read as “A:::::11:::::11::11A”, indicating that all oligonucleotides are recognized as bars and all blank controls are recognized as spaces.

Limit of Quantitation. We can determine the limit of quantitation (LOQ)³⁴ of assays in the barcoded microchip by gradient dilution of the specimen to be tested (Figure 6; see the Supporting Information for the protocol of determination of LOQ). The sample volume for each channel is 1 μ L. For serially diluted samples, the LOQ is defined as the lowest concentration at which the result is positive (recognized as a bar), and the corresponding symbol is read as “:”, while a concentration lower than this value yields a negative result (recognized as a space), and the corresponding symbol is read as “1”. For demonstration, the serially diluted target molecules (1 μ M to 1 pM), HBV-specific oligonucleotides, are introduced into C2–C15. Each concentration has four parallels. The result is read as “A::::::::::11111111A” (Figure 6). This barcode denotes that the LOQ for HBV is 10 pM, since the corresponding region of 10 pM target is read as “:” and the corresponding region of 1 pM is read as “1”. The LOQ of 10 pM for HBV detection by the barcoded microchip is comparable to that of existing microarray technology. To semiquantify a specific target with unknown concentration, we can first serially dilute the sample in the same way, determine the dilution factor below which the assay result is negative, and multiply the dilution factor by the specific threshold value (i.e., LOQ).

Coding Capacity of Barcoded Microchips. The coding capacity is defined as 2^n , where “ n ” is the sample size as well as the number of paired channels. For $n = 20$, the coding capacity is $2^{20} \approx 1$ million. The coding capacity of barcoded microchips is also

related to the size of a barcode, which can be shrunk according to the international symbology specification (Figure S2, Supporting Information). We find that the Codabar barcode can be interpreted even scaling down to 65% of the original size. If the widths of the elements of the barcode are decreased to 65% proportionally, the coding capacity will increase to $2^{n/0.65}$ if we use a chip with the original size. For $n = 20$, the coding capacity will be increased to $2^{20/0.65} \approx 2^{31} \approx 2$ billion. This coding capacity is comparable with that of color-coded microparticles ($2^{30} \approx 1$ billion)¹⁶ and 3 orders of magnitude higher than that of binary dot-coded particles for multiplexed bioassays.²⁴ Keeping the same coding capacity, this feature will also help to miniaturize the size of the device, thus further reducing the sample/reagent consumption.

In addition, the Codabar barcode does not limit the number of symbols, so researchers can achieve essentially arbitrary throughput. Correspondingly, there are some barcode readers that can support barcodes composed of more symbols (e.g., up to 74 symbols, barcode reader BL-1300 series, Keyence) and realize even more multiplexed assays. The throughput of this system can be easily controlled due to our flexible and expandable microfluidic design.

CONCLUSION

In conclusion, here we developed a barcoded microchip with a huge coding capacity that is compatible with various existing types of bioassays. We can call our strategy “positional encoding”, because the physical positions of chemical reactions are important and provide the key information for pattern encoding and recognition. This design allows not only a barcode reader, but also an electronic device equipped with a digital camera such as a smartphone for readout. The strategy for information encoding and decoding described here may give a great opportunity for other analytical applications.

ASSOCIATED CONTENT

Supporting Information

Additional information as noted in text. This material is available free of charge via the Internet at <http://pubs.acs.org>.

AUTHOR INFORMATION

Corresponding Authors

*E-mail: xingyujiang@nanoctr.cn.

*E-mail: sunjs@nanoctr.cn.

*E-mail: zhangw@nanoctr.cn.

Notes

The authors declare no competing financial interest.

ACKNOWLEDGMENTS

We acknowledge financial support from the Ministry of Science and Technology (MOST) (Grants 2013AA032204 and 2013YQ190467), National Natural Science Foundation of China (NSFC) (Grants 21475028, S1105086, 21025520, and 81361140345), Beijing Municipal Science & Technology Commission (Grant Z131100002713024), Chinese Academy of Sciences (Grants XDA09030305 and XDA09030308), and State Administration of Foreign Experts Affairs of the Chinese Academy of Sciences (CAS/SAFEA) International Partnership Program for Creative Research Teams.

REFERENCES

- (1) Sun, J.; Xianyu, Y.; Jiang, X. *Chem. Soc. Rev.* 2014, 43, 6239–6253.

- (2) Zhang, Y.; Guo, Y. M.; Xianyu, Y. L.; Chen, W. W.; Zhao, Y. Y.; Jiang, X. Y. *Adv. Mater.* **2013**, *25*, 3802–3819.
- (3) Sun, J.; Gao, Y.; Isaacs, R. J.; Boelte, K. C.; Lin, C. P.; Boczek, E. M.; Li, D. *Anal. Chem.* **2012**, *84*, 2017–2024.
- (4) Zhang, Y.; Zhang, L.; Sun, J.; Liu, Y.; Ma, X.; Cui, S.; Ma, L.; Xi, J.; Jiang, X. *Anal. Chem.* **2014**, *7057*–7062.
- (5) Pan, W. Y.; Chen, W.; Jiang, X. Y. *Anal. Chem.* **2010**, *82*, 3974–3976.
- (6) Xiong, B.; Ren, K.; Shu, Y.; Chen, Y.; Shen, B.; Wu, H. *Adv. Mater.* **2014**, *26*, 5525–5532.
- (7) Zhang, L.; Zhang, Y.; Wang, C.; Feng, Q.; Fan, F.; Zhang, G.; Kang, X.; Qin, X.; Sun, J.; Li, Y.; Jiang, X. *Anal. Chem.* **2014**, *86*, 10461–10466.
- (8) He, S.; Zhang, Y.; Wang, P.; Xu, X.; Zhu, K.; Pan, W.; Liu, W.; Cai, K.; Sun, J.; Zhang, W.; Jiang, X. *Lab Chip* **2015**, *15*, 105–112.
- (9) Xiang, Y.; Lu, Y. *Nat. Chem.* **2011**, *3*, 697–703.
- (10) Nie, Z. H.; Deiss, F.; Liu, X. Y.; Akbulut, O.; Whitesides, G. M. *Lab Chip* **2010**, *10*, 3163–3169.
- (11) Fan, R.; Vermesh, O.; Srivastava, A.; Yen, B. K. H.; Qin, L. D.; Ahmad, H.; Kwong, G. A.; Liu, C. C.; Gould, J.; Hood, L.; Heath, J. R. *Nat. Biotechnol.* **2008**, *26*, 1373–1378.
- (12) Araz, M. K.; Apori, A. A.; Salisbury, C. M.; Herr, A. E. *Lab Chip* **2013**, *13*, 3910–3920.
- (13) Nicewarner-Peña, S. R.; Freeman, R. G.; Reiss, B. D.; He, L.; Pena, D. J.; Walton, I. D.; Cromer, R.; Keating, C. D.; Natan, M. J. *Science* **2001**, *294*, 137–141.
- (14) Qin, L. D.; Park, S.; Huang, L.; Mirkin, C. A. *Science* **2005**, *309*, 113–115.
- (15) Matthias, S.; Schilling, J.; Nielsch, K.; Muller, F.; Wehrspohn, R. B.; Gosele, U. *Adv. Mater.* **2002**, *14*, 1618–1621.
- (16) Lee, H.; Kim, J.; Kim, H.; Kwon, S. *Nat. Mater.* **2010**, *9*, 745–749.
- (17) Geiss, G. K.; Bumgarner, R. E.; Birditt, B.; Dahl, T.; Dowidar, N.; Dunaway, D. L.; Fell, H. P.; Ferree, S.; George, R. D.; Grogan, T.; James, J. J.; Maysuria, M.; Mitton, J. D.; Oliveri, P.; Osborn, J. L.; Peng, T.; Ratcliffe, A. L.; Webster, P. J.; Davidson, E. H.; Hood, L. *Nat. Biotechnol.* **2008**, *26*, 317–325.
- (18) Cunin, F.; Schmedake, T. A.; Link, J. R.; Li, Y. Y.; Koh, J.; Bhatia, S. N.; Sailor, M. J. *Nat. Mater.* **2002**, *1*, 39–41.
- (19) Han, M. Y.; Gao, X. H.; Su, J. Z.; Nie, S. *Nat. Biotechnol.* **2001**, *19*, 631–635.
- (20) Li, Y. G.; Cu, Y. T. H.; Luo, D. *Nat. Biotechnol.* **2005**, *23*, 885–889.
- (21) Steemers, F. J.; Ferguson, J. A.; Walt, D. R. *Nat. Biotechnol.* **2000**, *18*, 91–94.
- (22) Zhao, Y.; Shum, H. C.; Chen, H.; Adams, L. L. A.; Gu, Z.; Weitz, D. A. *J. Am. Chem. Soc.* **2011**, *133*, 8790–8793.
- (23) Park, K. M.; Kim, C.; Thomas, S. W.; Yoon, H. J.; Morrison, G.; Mahadevan, L.; Whitesides, G. M. *Adv. Mater.* **2011**, *23*, 4851–4856.
- (24) Pregibon, D. C.; Toner, M.; Doyle, P. S. *Science* **2007**, *315*, 1393–1396.
- (25) Mandecki, W.; Pappas, M. G.; Kogan, N.; Wang, Z. Y.; Zamlynny, B. In *Microfabricated Sensors: Applications of Optical Technology for DNA Analysis*; Kordal, R., Usmani, A., Law, W. T., Eds.; American Chemical Society: Washington, DC, 2002; pp 57–69.
- (26) Palacios, M. A.; Benito-Peña, E.; Manesse, M.; Mazzeo, A. D.; LaFratta, C. N.; Whitesides, G. M.; Walt, D. R. *Proc. Natl. Acad. Sci. U.S.A.* **2011**, *108*, 16510–16514.
- (27) Nicewarner-Peña, S. R.; Carado, A. J.; Shale, K. E.; Keating, C. D. *J. Phys. Chem. B* **2003**, *107*, 7360–7367.
- (28) Fournier-Bidoz, S.; Jennings, T. L.; Klostranec, J. M.; Fung, W.; Rhee, A.; Li, D.; Chan, W. C. W. *Angew. Chem., Int. Ed.* **2008**, *47*, 5577–5581.
- (29) Ly, N.; Tao, N. *Appl. Phys. Lett.* **2006**, *88*, 043901.
- (30) Qin, L. D.; Banholzer, M. J.; Millstone, J. E.; Mirkin, C. A. *Nano Lett.* **2007**, *7*, 3849–3853.
- (31) Banholzer, M. J.; Osberg, K. D.; Li, S.; Mangelson, B. F.; Schatz, G. C.; Mirkin, C. A. *ACS Nano* **2010**, *4*, 5446–5452.
- (32) Wang, J.; Zhou, Y.; Qiu, H.; Huang, H.; Sun, C.; Xi, J.; Huang, Y. *Lab Chip* **2009**, *9*, 1831–1835.
- (33) Nam, J. M.; Thaxton, C. S.; Mirkin, C. A. *Science* **2003**, *301*, 1884–1886.
- (34) Gershon, H.; Gershon, D. *Mech. Ageing Dev.* **2000**, *120*, 1–22.